Contribution from the Departments of Chemistry, University of Winnipeg, Winnipeg, Manitoba, Canada R3B 2E9, and University of Windsor, Windsor, Ontario, Canada N9B 3P4

Heterobimetallic Dicyclohexylphosphido-Bridged Complexes of MoNi, MoPd, MoPt, WNi, WPd, and WPt. Crystal and Molecular Structure of $\overline{(CO)_4Mo(\mu\text{-}PCy_2)_2Pd(PPh_3)}$

Stephen J. Loeb,[*1a] Hilary A. Taylor,[1a] Lucio Gelmini,[1b] and Douglas W. Stephan[*1b]

Received October 1, 1985

Reaction of PCy_2H with $cis\text{-}M(CO)_4(C_5H_{11}N)_2$ (2:1) results in the formation of $cis\text{-}M(CO)_4(PCy_2H)_2$ (M = Mo (**1**), W (**2**)). Generation of $Li_2[M(CO)_4(PCy_2)_2]$ in situ from the reaction of **1** and **2** with n-BuLi (1:2) and the addition to a suspension of $M'Cl_2(PPh_3)_2$ yields the dicyclohexylphosphido-bridged complexes $(CO)_4\overline{M(\mu\text{-}PCy_2)_2M'}(PPh_3)$ (M = Mo, M' = Ni (**3**), Pd (**4**), Pt (**5**); M = W, M' = Ni (**6**), Pd (**7**), Pt (**8**)). All the complexes were characterized by $^{31}P\{^1H\}$ NMR and IR spectroscopy. The crystal and molecular structure of $(CO)_4\overline{Mo(\mu\text{-}PCy_2)_2Pd}(PPh_3)$ (**4**) was determined. It crystallizes in the space group Cc with $a = 21.474 (4)$ Å, $b = 10.573 (1)$ Å, $c = 22.954 (4)$ Å, $\beta = 117.53 (1)°$, $V = 4621 (1)$ Å^3, and $Z = 4$. The structure was refined to final $R = 0.0341$ and $R_w = 0.0375$ for 3566 reflections with $F_o^2 > 3\sigma(F_o^2)$. The Mo atom has pseudooctahedral geometry, coordinated to two bridging PCy_2 groups and four CO's. The Pd center has pseudo-trigonal-planar geometry and is coordinated to two bridging PCy_2 ligands and a terminal PPh_3 group. The Mo–Pd distance is 2.760 (1) Å, implying a metal–metal bond, and the $MoPd(\mu\text{-}PCy_2)_2$ dihedral angle is 15.4°, reflecting steric interactions between phenyl and cyclohexyl groups.

Introduction

Heteronuclear metal–metal-bonded complexes are of current interest because unique chemical reactivity may result from linking together metals with different substrate reactivity.[2] Di- and polynuclear complexes that contain bridging ligands such as diorganophosphido groups are particularly desirable since these ligands may prevent rearrangement of the metal centers during reactions.[3,4]

The combination of increased basicity and steric bulk of large trialkylphosphine ligands is well-known to affect the reactivity of transition-metal complexes.[5] However, analogous studies on the effect of sterically demanding dialkylphosphido bridging ligands are limited.[6] Geoffroy and others have prepared a number of interesting metal combinations (WPt,[3c] FeRh,[3b] WRe,[3h] WOs,[4a] TiW,[3f] ThNi,[3i] and MoZr,[3j] for example), but the majority of these contain the diphenylphosphido ligand. Jones has studied the steric effects of the di-*tert*-butylphosphido ligand and shown that the increased steric requirements of the *t*-Bu groups are important and the resulting chemistry is different from that generally observed for the smaller ligands.[6,7]

In this paper, we report our initial investigations into the use of dicyclohexylphosphido-bridging ligands in heterobimetallic complexes. At present, very few dicyclohexylphosphido-bridged complexes appear in the literature, $[Ni(\mu\text{-}PCy_2)(PCy_2Ph)_2]_2$,[8] $[Ni(\mu\text{-}PCy_2)(CO)_2]_2$,[8] and $ZrFe(\mu\text{-}PCy_2)_2Cp_2(CO)_3$,[3f] and none have been structurally characterized by X-ray diffraction. The "bridge-assisted" synthetic method has been used to prepare complexes of the general formula $(CO)_4\overline{M(\mu\text{-}PCy_2)_2M'}(PPh_3)$ (M = Mo, W; M' = Ni, Pd, Pt) (eq 1). The synthesis and

$$Li_2[(CO)_4M(PCy_2)_2] + M'Cl_2(PPh_3)_2 \rightarrow$$

$$(CO)_4\overline{M(\mu\text{-}PCy_2)_2M'}(PPh_3) + 2LiCl + PPh_3 \quad (1)$$

characterization of this series of complexes is described along with an X-ray crystal structure of the MoPd complex.

Experimental Section

$PdCl_2(PPh_3)_2$,[9] $cis\text{-}PtCl_2(PPh_3)_2$,[9] $NiCl_2(PPh_3)_2$,[10] $cis\text{-}Mo(CO)_4(C_5H_{11}N)_2$,[11] and $cis\text{-}W(CO)_4(C_5H_{11}N)_2$[11] ($C_5H_{11}N$ = piperidine) were prepared by literature methods. $NiCl_2\cdot 6H_2O$ (Baker), $Mo(CO)_6$, $W(CO)_6$, K_2PtCl_4, PCy_2H, K_2PdCl_4 (Strem), n-BuLi, and PPh_3 (Aldrich) were purchased and used as received. THF (tetrahydrofuran) and toluene were dried by distillation from Na–benzophenone ketyl under N_2; CH_2Cl_2 was dried by distillation from P_2O_5 under N_2; n-hexane was dried over molecular sieves and degassed with N_2 prior to use. All reactions were conducted under an atmosphere of N_2 by standard Schlenk techniques.[12]

^{31}P NMR spectra were obtained at 36.4 MHz on a Bruker WH-90 spectrometer at 300 K with an external D_2O lock. Phosphorus chemical shifts were measured relative to external 85% H_3PO_4 with positive shifts downfield. Infrared spectra were recorded on a Perkin-Elmer 781 grating spectrometer.

Preparation of *cis*-Mo(CO)$_4$(PCy$_2$H)$_2$ (1). PCy_2H (7.51 mL, 36.4 mmol) was added to a suspension of $cis\text{-}Mo(CO)_4(C_5H_{11}N)_2$ (6.37 g, 18.2 mmol) in 40 mL of toluene. The mixture was stirred overnight at room temperature and the solvent removed in vacuo. The resultant off-white solid was washed with 2 × 10 mL of cold diethyl ether and

(1) (a) University of Winnipeg. (b) University of Windsor.
(2) (a) Roberts, D. A.; Geoffroy, G. L. In *Comprehensive Organometallic Chemistry*; Wilkinson, G., Stone, F. G. A., Abel, E., Eds.; Pergamon: Oxford, England, 1982; Chapter 40. (b) Barger, P. T.; Bercaw, J. E. *Organometallics* **1984**, *3*, 278. (c) Finke, R. G.; Gaughan, G.; Pierpoint, C.; Noordik, J. H. *Organometallics* **1983**, *2*, 1481. (d) Casey, C. P.; Bullock, R. M.; Nief, F. *J. Am. Chem. Soc.* **1983**, *105*, 7574. (e) White, G. L.; Stephan, D. W. *Inorg. Chem.* **1985**, *24*, 1499.
(3) (a) Breen, M. J.; Geoffroy, G. L. *Organometallics* **1982**, *1*, 1437. (b) Roberts, D. A.; Steinmetz, G. R.; Breen, M. J.; Shulman, P. M.; Morrison, E. D.; Duttera, M. R.; De Brosse, C. W.; Whittle, R. R.; Geoffroy, G. L. *Organometallics* **1983**, *2*, 846. (c) Morrison, E. D.; Harley, A. D.; Marcelli, M. A.; Geoffroy, G. L.; Rheingold, A. L.; Fultz, W. C. *Organometallics* **1984**, *3*, 1407. (d) Chandler, D. J.; Jones, R. A.; Stuart, A. L.; Wright, T. C. *Organometallics* **1984**, *3*, 1830. (e) Jones, R. A.; Lasch, J. G.; Norman, N. C.; Stuart, A. L.; Wright, T. C.; Whittlesey, B. R. *Organometallics* **1984**, *3*, 114. (f) Targos, T. S.; Rosen, R. P.; Whittle, R. R.; Geoffroy, G. L. *Inorg. Chem.* **1985**, *24*, 1375. (g) Baker, R. T.; Tulip, T. H.; Wreford, S. S. *Inorg. Chem.* **1985**, *24*, 1379. (h) Mercer, W. C.; Whittle, R. R.; Burkhardt, E. W.; Geoffroy, G. L. *Organometallics* **1985**, *4*, 68. (i) Ritchy, J. M.; Zozulin, A. J.; Wrobleski, D. A.; Ryan, R. R.; Wasserman, H. J.; Moody, D. C.; Paine, R. T. *J. Am. Chem. Soc.* **1985**, *107*, 501. (j) Gelmini, L.; Matassa, L. C.; Stephan, D. W. *Inorg. Chem.* **1985**, *24*, 2585.
(4) Phosphido ligands are not always inert and unreactive. (a) Geoffroy, G. L.; Rosenberg, S.; Shulman, P. M.; Whittle, R. R. *J. Am. Chem. Soc.* **1984**, *106*, 1519. (b) Crowte, R. J.; Evans, J. *J. Chem. Soc., Chem. Commun.* **1984**, 1332.
(5) Tolman, C. A. *Chem. Rev.* **1977**, *77*, 313.
(6) See ref 3d,e and: Jones, R. A.; Stuart, A. L.; Atwood, J. L.; Hunter, W. E.; Rogers, R. D. *Organometallics* **1982**, *1*, 1721.

(7) (a) Jones, R. A.; Wright, T. C.; Atwood, J. L.; Hunter, W. E. *Organometallics* **1983**, *2*, 470. (b) Jones, R. A.; Wright, T. C. *Organometallics* **1983**, *2*, 1842. (c) Atwood, J. L.; Hunter, W. E.; Jones, R. A.; Wright, T. C. *Inorg. Chem.* **1983**, *22*, 993.
(8) Nobile, F.; Varapollo, G.; Giannoccaro, P.; Sacco, A. *Inorg. Chim. Acta* **1981**, *48*, 261.
(9) Bailar, J. C., Jr.; Itanani, H. *Inorg. Chem.* **1965**, *4*, 1618. ($PdCl_2(PPh_3)_2$ is prepared by the same method, producing a yellow crystalline solid in 75% yield.)
(10) Venanzi, L. M. *J. Chem. Soc.* **1958**, 719.
(11) Darensbourg, D. J.; Kump, R. L. *Inorg. Chem.* **1978**, *17*, 2680.
(12) Shriver, D. F. *The Manipulation of Air-Sensitive Compounds*; Mcgraw-Hill: New York, 1969.

dried in vacuo, yielding 7.81 g (71%). ^{31}P NMR (CH$_2$Cl$_2$): δ 25.9 (d, J_{PH} = 301.1 Hz). Anal. Calcd for C$_{28}$H$_{46}$MoO$_4$P$_2$: C, 55.62; H, 7.68. Found: C, 56.02; H, 7.48.

Preparation of *cis*-W(CO)$_4$(PCy$_2$H)$_2$ (2). PCy$_2$H (3.08 mL, 14.9 mmol) was added to a suspension of *cis*-W(CO)$_4$(C$_5$H$_{11}$N)$_2$ (3.21 g, 7.45 mmol) in 30 mL of toluene. The mixture was stirred with warming (ca. 60 °C) for 4 h, cooled to room temperature, and filtered and the solvent removed in vacuo. The resulting bright yellow solid was recrystallized from toluene, yielding 3.51 g (68%). ^{31}P NMR (CH$_2$Cl$_2$): δ 10.0 (d of t, J_{PH} = 312.6 Hz, J_{WP} = 214.5 Hz). Anal. Calcd for C$_{28}$H$_{46}$O$_4$P$_2$W: C, 48.56; H, 6.71. Found: C, 48.71; H, 6.66.

Preparation of (CO)$_4$Mo(μ-PCy$_2$)$_2$Ni(PPh$_3$) (3). *n*-Butyllithium (1.55 M in hexanes, 5.38 mL, 8.34 mmol) was added via syringe to a THF (20 mL) solution of 1 (2.52 g, 4.17 mmol) at 23 °C. After it was stirred 10 min, this solution was added dropwise, over 30 min, to a suspension of NiCl$_2$(PPh$_3$)$_2$ (2.73 g, 4.17 mmol) in 30 mL of THF at 0 °C. An immediate color change from green to dark orange was observed. The solution was warmed to room temperature and stirred for 2 h and the solvent removed in vacuo. The resulting dark orange-red solid was extracted with cold *n*-hexane (6 × 10 mL) and cooled at -20 °C for 8 h. The orange-red microcrystalline product was isolated by keeping the recrystallization flask at ca. -10 °C, removing the mother liquor, and drying the solid in vacuo. (If the solution is warmed to room temperature during the isolation process, only brown oily products result.) This yielded 2.15 g of 3 (56%). Anal. Calcd for C$_{46}$H$_{59}$MoNiO$_4$P$_3$: C, 59.93; H, 6.46. Found: C, 59.39; H, 6.45.

Preparation of (CO)$_4$Mo(μ-PCy$_2$)$_2$Pd(PPh$_3$) (4). *n*-Butyllithium (1.55 M in hexanes, 2.67 mL, 4.14 mmol) was added via syringe to a THF (20 mL) solution of 1 (1.18 g, 2.07 mmol) at 23 °C. After it was stirred for 10 min, this solution was added dropwise, over 30 min, to a suspension of PdCl$_2$(PPh$_3$)$_2$ (1.40 g, 2.07 mmol) in 30 mL of THF at 0 °C. The resulting dark red solution was stirred at room temperature for 4 h and the solvent removed in vacuo. The residue was extracted with *n*-hexane (7 × 10 mL) and the solution volume reduced to 40 mL. After the solution was cooled at -20 °C for 12 h red crystals of 4 were isolated; yield 0.99 g (48%). Anal. Calcd for C$_{46}$H$_{59}$MoO$_4$P$_3$Pd: C, 56.88; H, 6.14. Found: C, 57.01; H, 6.23.

Preparation of (CO)$_4$Mo(μ-PCy$_2$)$_2$Pt(PPh$_3$) (5). *n*-Butyllithium (1.55 M in hexanes, 0.65 mL, 1.01 mmol) was added via syringe to a THF (20 mL) solution of 1 (0.31 g, 0.51 mmol) at 23 °C. After it was stirred for 10 min, this solution was added dropwise, over 30 min, to a suspension of *cis*-PtCl$_2$(PPh$_3$)$_2$ (0.40 g, 0.51 mmol) in 30 mL of THF at 23 °C. The resulting dark orange solution was stirred for 24 h at room temperature and the solvent removed in vacuo. The residue was extracted with *n*-hexane (5 × 10 mL) and the volume of the solution reduced to 20 mL. After the solution was cooled at -20 °C for 36 h, orange microcrystals of 5 were isolated, yield 0.22 g (41%). Anal. Calcd for C$_{46}$H$_{59}$MoO$_4$P$_3$Pt: C, 52.10; H, 5.62. Found: C, 52.44; H, 5.57.

Preparation of (CO)$_4$W(μ-PCy$_2$)$_2$Ni(PPh$_3$) (6). *n*-Butyllithium (1.55 M in hexanes, 3.73 mL, 5.78 mmol) was added via syringe to a THF (20 mL) solution of 2 (2.00 g, 2.89 mmol) at 23 °C. After it was stirred for 10 min, this solution was added dropwise, over 30 min, to a suspension of NiCl$_2$(PPh$_3$)$_2$ (1.89 g, 2.89 mmol) in 30 mL of THF at 0 °C. The dark red-orange solution was warmed to room temperature and stirred for 3 h. The solvent was removed in vacuo, and the solid residue was extracted with *n*-hexane (4 × 10 mL). After the solution volume was reduced slightly and the solution was cooled at -20 °C for 10 h, red-brown microcrystals of 6 were isolated; yield 1.75 g (60%). This procedure was performed at -10 °C as for 3. Anal. Calcd for C$_{46}$H$_{59}$NiO$_4$P$_3$W: C, 54.71; H, 5.90. Found: C, 54.72; H, 5.82.

Preparation of (CO)$_4$W(μ-PCy$_2$)$_2$Pd(PPh$_3$) (7). *n*-Butyllithium (1.55 M in hexanes, 3.16 mL, 4.90 mmol) was added via syringe to a THF (20 mL) solution of 2 (1.70 g, 2.45 mmol) at 23 °C. After it was stirred for 10 min, this solution was added dropwise, over 30 min, to a suspension of PdCl$_2$(PPh$_3$)$_2$ (1.72 g, 2.45 mmol) in 30 mL of THF at 0 °C. The dark orange-red solution was warmed to room temperature and stirred for 6 h. The THF was removed in vacuo and the solid residue extracted with *n*-hexane (6 × 10 mL). The solution was filtered and the volume reduced to 30 mL. After the solution was cooled at -20 °C for 12 h, orange-red crystals were isolated; yield 1.14 g (44%). Anal. Calcd for C$_{46}$H$_{59}$O$_4$P$_3$PdW: C, 52.14; H, 5.62. Found: C, 52.00; H, 5.71.

Preparation of (CO)$_4$W(μ-PCy$_2$)$_2$Pt(PPh$_3$) (8). *n*-Butyllithium (1.55 M in hexanes, 0.64 mL, 0.99 mmol) was added via syringe to a THF (40 mL) solution of 2 (0.34 g, 0.49 mmol) at 23 °C. After it was stirred for 10 min, the solution was added dropwise, over 15 min, to a suspension of *cis*-PtCl$_2$(PPh$_3$)$_2$ (0.39 g, 0.49 mmol) in 15 mL of THF at 23 °C. The dark orange-brown solution was stirred for 19 h at room temperature.

Table I. Summary of Crystal Data, Intensity Collection, and Structure Refinement for (CO)$_4$Mo(μ-PCy$_2$)$_2$Pd(PPh$_3$) (4)

formula	MoPdP$_3$O$_4$C$_{45}$H$_{59}$
cryst color, form	red-orange, blocks
a, Å	21.474 (4)
b, Å	10.573 (1)
c, Å	22.954 (4)
β, deg	117.53 (1)
cryst syst	monoclinic
space group	Cc
vol, Å^3	4621 (1)
ρ(calcd), g/cm^3	1.40
Z	4
cryst dimens, mm	0.27 × 0.46 × 0.96
μ, abs coeff, cm^{-1}	7.17
radiation (λ, Å)	Mo Kα (0.710 69)
temp, °C	24
scan speed, deg/min	2.0–5.0 ($\theta/2\theta$ scan)
scan range, deg	1.0 below K$_1$ to 1.1 above K$_2$
bkgd/scan time ratio	0.5
data collected	6570; 2θ of 4.5 to 50° (+h,+k,±l)
unique data ($F_o^2 > 3\sigma F_o^2$)	3566
no. of variables	370 (2 blocks)
R, %	3.41
R_w, %	3.75

The THF was removed in vacuo and the orange-brown residue extracted with *n*-hexane (7 × 5 mL). The volume of the solution was reduced to 5 mL, and orange microcrystals formed after cooling at -20 °C for 16 h; yield 0.240 g (42%). Anal. Calcd for C$_{46}$H$_{59}$O$_4$P$_3$PtW: C, 48.11; H, 5.19. Found: C, 48.33; H, 5.09.

X-ray Diffraction Study of 4. Crystallization of 4 was achieved by maintaining a *n*-hexane solution of the complex at -20 °C for 48 h. A suitable red crystal of 4 was encapsulated in a glass capillary under N$_2$. Diffraction experiments were performed on a four-circle Syntex P2$_1$ diffractometer with graphite-monochromatized Mo Kα radiation. An initial orientation matrix was obtained from 15 machine-centered reflections selected from rotation photographs. Partial rotation photographs around each axis were consistent with a monoclinic crystal system. Ultimately, 30 high-angle reflections (13° < 2θ < 37°) were used to obtain the final lattice parameters and orientation matrix. Machine parameters, crystal data, and data collection parameters are summarized in Table I. The observed extinctions were consistent with space groups Cc and $C2/c$. Cc was confirmed by a successful structure refinement. Intensity data (+h,+k,±l) were collected in two shells (4.5° < 2θ < 45.0° and 45.0° < 2θ < 50.0°). The intensities of 3 standard reflections were collected every 197 reflections and showed no statistically significant change over the duration of the data collection. No absorption correction was applied to the data (μ = 7.17 cm^{-1}). The data were processed by using the SHELX-76 program package on the computing facilities at the University of Windsor. A total of 3566 reflections with $F_o^2 > 3\sigma(F_o^2)$ were used in the refinement.

The Mo and Pd atom positions were located in a Patterson synthesis, and the remaining non-hydrogen atoms were located from successive difference Fourier map calculations. Refinement was carried out by using full-matrix least-squares techniques on F minimizing the function $\sum w(|F_o| - |F_c|)^2$, where $w = 4F_o^2/\sigma^2(F_o^2)$ and F_o and F_c are the observed and calculated structure factor amplitudes. Atomic scattering factors[13] and anomalous dispersion terms[14] were taken from the usual sources. In the first cycles of least-squares refinement, all non-hydrogen atoms, with exception of the phenyl C atoms, were assigned anisotropic thermal parameters. Fixed H atom contributions were included with C–H distances of 0.95 Å and thermal parameters equal to 1.10 times the isotropic thermal parameter of the bonded C atoms. The phenyl rings were constrained to an idealized D_{6h} symmetry with C–C distances of 1.39 Å. This resulted in

$$R = \sum ||F_o| - |F_c||/\sum |F_o| = 0.0341$$

$$R_w = (\sum w(|F_o| - |F_c|)^2/\sum w|F_o|)^{1/2} = 0.0375$$

at final convergence. The maximum Δ/σ value on any of the parameters in the final cycles was 0.151 associated with the thermal parameter of

(13) Cromer, D. T.; Waber, J. T. *International Tables for X-ray Crystallography*; Kynoch: Birmingham, England, 1974.

(14) (a) Cromer, D. T.; Mann, J. B. *Acta Crystallogr., Sect. A: Cryst. Phys., Diffr., Theor. Gen. Crystallogr.* **1968**, *A24*, 321. (b) *Ibid.* **1968**, *A24*, 390.

Table II. Selected Bond Distances and Angles

Distances (Å)

Mo–Pd	2.760 (1)	P1–C41	1.85 (1)	Mo–C2	2.027 (9)
Mo–P1	2.530 (1)	P2–C11	1.859 (7)	Mo–C3	2.027 (8)
Mo–P2	2.542 (2)	P2–C21	1.86 (1)	Mo–C4	2.051 (7)
Pd–P1	2.287 (2)	P3–C51	1.839	C1–O1	1.14 (1)
Pd–P2	2.267 (2)	P3–C61	1.848 (6)	C2–O2	1.12 (1)
Pd–P3	2.280 (2)	P3–C71	1.819 (6)	C3–O3	1.13 (1)
P1–C31	1.85 (1)	Mo–C1	2.00 (1)	C4–O4	1.126 (9)

Angles (deg)

P1–Pd–P2	118.7 (1)	P1–Pd–P3	118.5 (1)	P2–Pd–P3	122.3 (1)
P1–Mo–P2	101.2 (1)	P1–Mo–C1	170.9 (3)	P1–Mo–C2	87.7 (3)
P1–Mo–C3	84.7 (3)	P1–Mo–C4	93.8 (3)	P2–Mo–C1	82.0 (3)
P2–Mo–C2	170.3 (2)	P2–Mo–C3	94.0 (2)	P2–Mo–C4	91.7 (2)
C1–Mo–C2	89.9 (4)	C1–Mo–C3	86.6 (4)	C1–Mo–C4	94.6 (4)
C2–Mo–C3	90.8 (3)	C2–Mo–C4	83.6 (3)	C3–Mo–C4	174.3 (3)
Mo–P1–Pd	69.7 (1)	Mo–P1–C31	123.4 (3)	Mo–P1–C41	118.2 (4)
Mo–P2–Pd	69.8 (1)	Mo–P2–C11	117.6 (2)	Mo–P2–C21	120.8 (2)
Pd–P1–C31	117.1 (3)	Pd–P1–C41	121.4 (4)	Pd–P2–C11	119.1 (3)
Pd–P2–C21	125.9 (2)	Pd–P3–C51	121.5 (1)	Pd–P3–C61	118.8 (2)
Pd–P3–C71	105.9 (2)	C51–P3–C61	100.4 (2)	C51–P3–C71	103.3 (2)
C61–P3–C71	105.1 (3)				

Table III. Positional Parameters[a]

atom	x	y	z	atom	x	y	z
Mo	0 (0)	1554 (1)	7500 (0)	C31	1476 (5)	2215 (9)	7022 (4)
Pd	1177 (1)	2842 (1)	8384 (1)	C32	1378 (6)	3650 (9)	6975 (5)
P1	2134 (1)	1510 (2)	7625 (1)	C33	1666 (7)	4221 (12)	6528 (5)
P2	112 (1)	3267 (1)	8320 (1)	C34	1305 (7)	3651 (11)	5854 (5)
P3	2199 (1)	3492 (2)	9247 (1)	C35	1366 (9)	2229 (11)	5880 (6)
C1	–938 (4)	1323 (9)	7471 (4)	C36	1093 (7)	1652 (10)	6323 (4)
C2	–264 (4)	266 (9)	6770 (4)	C41	1728 (5)	5 (9)	7873 (5)
C3	347 (4)	161 (7)	8184 (4)	C42	2443 (7)	41 (14)	8263 (9)
C4	–354 (4)	2831 (7)	6742 (3)	C43	2825 (6)	–1154 (12)	8550 (5)
O1	–1443 (3)	1143 (9)	7506 (4)	C44	2555 (9)	–2296 (14)	8144 (9)
O2	–423 (4)	–410 (7)	6348 (3)	C45	1847 (10)	–2328 (13)	7729 (10)
O3	528 (4)	–650 (6)	8544 (3)	C46	1428 (5)	–1133 (9)	7439 (5)
O4	–593 (4)	3423 (7)	6282 (3)	C51	2342 (2)	5155 (4)	9513 (2)
C11	–310 (4)	4819 (6)	7987 (3)	C52	3015 (2)	5634 (4)	9897 (2)
C12	46 (4)	5539 (7)	7642 (4)	C53	3103 (2)	6882 (4)	10118 (2)
C13	–292 (6)	6823 (10)	7396 (6)	C54	2517 (2)	7651 (4)	9955 (2)
C15	–1082 (7)	6670 (10)	6944 (6)	C55	1844 (2)	7172 (4)	9571 (2)
C15	–1435 (5)	6028 (9)	7594 (5)	C56	1756 (2)	5923 (4)	9350 (2)
C16	–1103 (4)	4729 (7)	7530 (4)	C61	3037 (2)	3147 (5)	9235 (2)
C21	–153 (4)	2958 (7)	8974 (4)	C62	3141 (2)	3715 (2)	8738 (2)
C22	203 (5)	3882 (9)	9545 (4)	C63	3762 (2)	3498 (5)	8700 (2)
C23	–25 (6)	3623 (10)	10088 (5)	C64	4279 (2)	2716 (5)	9159 (2)
C24	115 (6)	2290 (11)	10316 (5)	C65	4176 (2)	2150 (2)	9657 (2)
C25	–236 (7)	1377 (10)	9766 (6)	C66	3555 (2)	2365 (5)	9695 (2)
C26	–26 (6)	1602 (8)	9211 (5)	C72	2441 (3)	3262 (4)	10562 (2)
C71	2255 (3)	2662 (4)	9963 (2)	C75	2192 (3)	1345 (4)	10988 (2)
C73	2410 (3)	2604 (4)	11074 (2)	C76	2037 (3)	1402 (4)	9877 (2)
C75	2006 (3)	743 (4)	10389 (2)				

[a] Multiplied by 10^4.

C42. This relatively large shift appears to be a result of the motion of cyclohexyl ring 4. The Δ/σ shifts for the remainder of the molecule were less than 0.020. A final difference Fourier map calculation showed no peaks of chemical significance; the largest was 0.76 e/Å³ associated with the Mo atom. Selected bond lengths and angles are summarized in Table II and atomic positional and thermal parameters in Table III. Anisotropic thermal parameters (Table S-I), hydrogen atom parameters (Table S-II), angles and distances associated with phenyl and cyclohexyl rings (Table S-III), and values of $10|F_o|$ and $10|F_c|$ (Table S-IV) are deposited as supplementary material.

Results and Discussion

Synthesis and Characterization of Complexes 1–8. A slight modification of the method of Darensbourg and Kump[11] was used to prepare the complexes cis-Mo(CO)₄(PCy₂H)₂ (**1**) and cis-W-(CO)₄(PCy₂H)₂ (**2**) in good yields (eq 2). Both **1** and **2** showed

cis-M(CO)₄(C₅H₁₁N)₂ + 2PCy₂H →

cis-M(CO)₄(PCy₂H)₂ + 2C₅H₁₁N   (2)

1: M = Mo (71%)
2: M = W (68%)
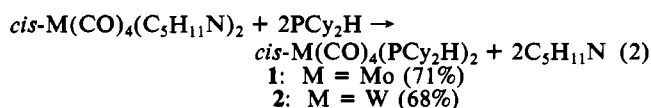
Table IV. Infrared Spectral Data

complex	ν_{CO},[a] cm⁻¹
cis-Mo(CO)₄(PCy₂H)₂ (**1**)	2018 (s),[b] 1923 (s), 1903 (vs), 1875 (sh)
cis-W(CO)₄(PCy₂H)₂ (**2**)	2014 (s), 1920 (s), 1896 (vs), 1872 (m)
MoNi (**3**)	2021 (s), 1943 (m, sh), 1928 (s), 1910 (vs, br)
MoPd (**4**)	2025 (s), 1955 (m), 1947 (m), 1919 (vs)
MoPt (**5**)	2029 (s), 1949 (m), 1925 (m), 1904 (s)
WNi (**6**)	2015 (s), 1935 (m, sh), 1917 (m), 1894 (br, vs)
WPd (**7**)	2024 (s), 1949 (m), 1940 (m), 1910 (vs)
WPt (**8**)	2022 (s), 1948 (m), 1939 (m), 1910 (vs)

[a] All in hexane solutions. [b] Abbreviations: s = strong, v = very, br = broad, m = medium, sh = shoulder.
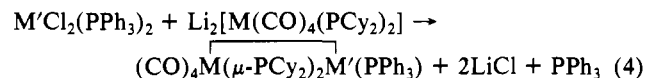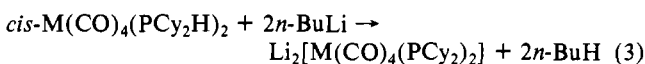
Table V. $^{31}P\{^1H\}$ NMR Spectral Data[a]

complex	$\delta(\mu\text{-PCy}_2)$	$\delta(\text{PPh}_3)$	$^2J_{PP}$, Hz	J_{MP}, Hz
MoNi (3)	210.5 (d)[b]	43.9 (t)	34.0	
MoPd (4)	261.2 (d)	37.8 (t)	27.4	
MoPt (5)	259.6 (d)	48.8 (t)	60.0	2499.6 (μ-PCy$_2$, M = Pt), 5238.6 (PPh$_3$, M = Pt)
WNi (6)	184.6 (d)	42.3 (t)	27.8	151.0 (μ-PCy$_2$, M = W)
WPd (7)	228.8 (d)	35.4 (t)	18.7	156.9 (μ-PCy$_2$, M = W)
WPt (8)	228.5 (d)	46.4 (t)	49.4	140.5 (μ-PCy$_2$, M = W), 2413.3 (μ-PCy$_2$, M = Pt), 5121.2 (PPh$_3$, M = Pt)

[a] Recorded in CH$_2$Cl$_2$ solution. [b] Abbreviations: d = doublet, t = triplet.

a single resonance in the $^{31}P\{^1H\}$ NMR spectrum at 25.9 and 10.0 ppm respectively (J_{PH} = 301.1 and 312.6 Hz, respectively; J_{WP} = 214.5 Hz). Infrared spectra (Table IV) showed four ν(CO) absorptions consistent with C_{2v} symmetry and a cis geometry for these complexes.

The heterobimetallic complexes 3–8 were prepared via the reactions outlined in eq 3 and 4. This approach is known as the

$$cis\text{-M(CO)}_4(\text{PCy}_2\text{H})_2 + 2n\text{-BuLi} \rightarrow$$
$$\text{Li}_2[\text{M(CO)}_4(\text{PCy}_2)_2] + 2n\text{-BuH} \quad (3)$$

$$\text{M}'\text{Cl}_2(\text{PPh}_3)_2 + \text{Li}_2[\text{M(CO)}_4(\text{PCy}_2)_2] \rightarrow$$
$$\overline{(\text{CO)}_4\text{M}(\mu\text{-PCy}_2)_2\text{M}'(\text{PPh}_3)} + 2\text{LiCl} + \text{PPh}_3 \quad (4)$$

3: M = Mo, M' = Ni (56%)
4: M = Mo, M' = Pd (48%)
5: M = Mo, M' = Pt (41%)
6: M = W, M' = Ni (60%)
7: M = W, M' = Pd (44%)
8: M = W, M' = Pt (42%)

"bridge-assisted" method[2a] of metal–metal bond formation and has been used extensively by Geoffroy[2,3] and others[4,6,7] for the preparation of heterobimetallic complexes bridged by R$_2$P ligands. It is proposed that these reactions proceed by nucleophilic displacement of the anionic chloride ligand by the phosphido group.[3f]

A red-orange solution of Li$_2$[M(CO)$_4$(PCy$_2$)$_2$] in THF was added to a slurry of M'Cl$_2$(PPh$_3$)$_2$, also in THF, and in each reaction an immediate color change was observed, even at 0 °C. The reaction was assumed to be complete when the M'Cl$_2$(PPh$_3$)$_2$ complex was no longer present, resulting in a clear dark orange or red solution. All the complexes are extremely soluble in most organic solvents, including diethyl ether, toluene, and n-hexane and can be recrystallized in moderate to good yields by cooling a saturated n-hexane solution to –20 °C. The MoPd (4), MoPt (5), WPd (7), and WPt (8) complexes are air-stable in the solid state, but their solutions are air-sensitive, decomposing rapidly. The MoNi (3) and WNi (6) complexes are air-sensitive in the solid state and solution; however, both are quite thermally stable and can be isolated in good yield. This is in marked contrast to the Ph$_2$P-bridged complex $\overline{(\text{CO)}_4\text{W}(\mu\text{-PPh}_2)_2\text{Ni}(\text{PPh}_3)}$, which Geoffroy reported could only be obtained impure, in poor yield, and was too unstable for detailed study.[3c]

Infrared and $^{31}P\{^1H\}$ NMR spectral data are in Tables IV and V. As with other phosphido-bridged complexes, the $^{31}P\{^1H\}$ NMR spectra are very useful in assigning molecular structures.[3a,4] Each complex shows a down field resonance (doublet), due to two bridging PCy$_2$ ligands, and another resonance (triplet) due to a single terminal PPh$_3$ ligand. The two sets of resonances are well separated by ca. 140–225 ppm depending on the complex. The large downfield shift of the bridging ligands is probably indicative of a metal–metal bond.[15] Although this is not conclusive, literature data show that for most μ-PR$_2$ ligands bridging a metal–metal bond the phosphorus chemical shift is downfield (δ +50–300) and for the same ligands not bridging a metal–metal bond the resonances are further upfield (δ +50 to –200).[15] However, it has been suggested that since exceptions do occur,
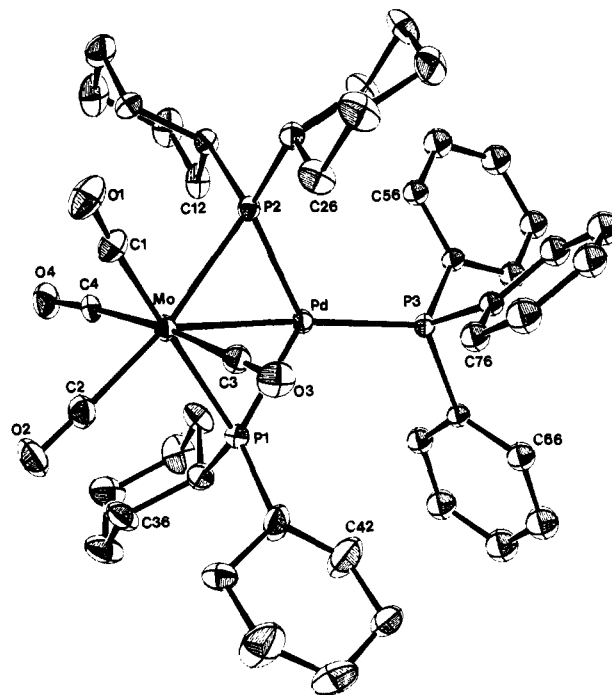
Figure 1. Perspective drawing of $\overline{(\text{CO)}_4\text{Mo}(\mu\text{-PCy}_2)_2\text{Pd}(\text{PPh}_3)}$ (4) showing the numbering scheme. The numbering of phenyl and cyclohexyl ring carbon atoms starts at the atom bound to phosphorus; 20% thermal ellipsoids are shown.

this type of correlation be made only for closely related series of compounds supported by X-ray crystallography, as in this work.[3f] The $^{31}P\{^1H\}$ NMR data also indicate that complexes 3–8 all have structures similar to that determined by X-ray diffraction for the MoPd complex 4 (Figure 1). Variations in chemical shifts within this series of compounds are presumably due to differences in electronic properties of the various metal centers. These trends are consistent with those found for mononuclear compounds[16] and those observed for related μ-PPh$_2$ complexes.[3c]

Infrared spectra of the heterobimetallic complexes 3–8 are very similar, each showing the expected four-band pattern in the terminal CO region, indicative of cis-M(CO)$_4$L$_2$, C_{2v}, geometry. The positions of these ν(CO) absorptions are shifted to significantly higher values (10–40 cm^{-1}) compared to those of the precursor, secondary phosphine complexes, indicative of a partial oxidation of the M(CO)$_4$ portion. This is interpreted as resulting from a M$^0 \rightarrow$ M$'^{II}$ dative metal–metal bond.

Crystal and Molecular Structure of $\overline{(\text{CO)}_4\text{Mo}(\mu\text{-PCy}_2)_2\text{Pd}\text{-}(\text{PPh}_3)}$ **(4).** A perspective view of 4 giving the atom-numbering scheme is shown in Figure 1, and a representation of the inner coordination sphere of the molecule is shown, with some relevant parameters, in Figure 2. The unit cell contains four discrete molecules of 4. The closest intermolecular nonbonded contact is 2.356 Å between cyclohexyl hydrogens H23B and H34B. Complete listings of interatomic distances and angles may be found in Tables II and S-III.

(15) (a) Peterson, J. L.; Stewart, R. P., Jr. *Inorg. Chem.* **1980**, *19*, 186. (b) Carty, A. J.; MacLaughlin, S. A.; Taylor, N. J. *J. Organomet. Chem.* **1981**, *204*, C27. (c) Carty, A. J. *Catalytic Aspects of Metal Phosphine Complexes*: Advances in Chemistry 196; American Chemical Society: Washington, DC, 1982; p 163.

(16) Pregosin, P. S.; Kunz, R. W. *Phosphorus-31 and Carbon-13 Nuclear Magnetic Resonance Studies of Transition Metal Complexes Containing Phosphorus Ligands*; Springer-Verlag: New York, 1979.
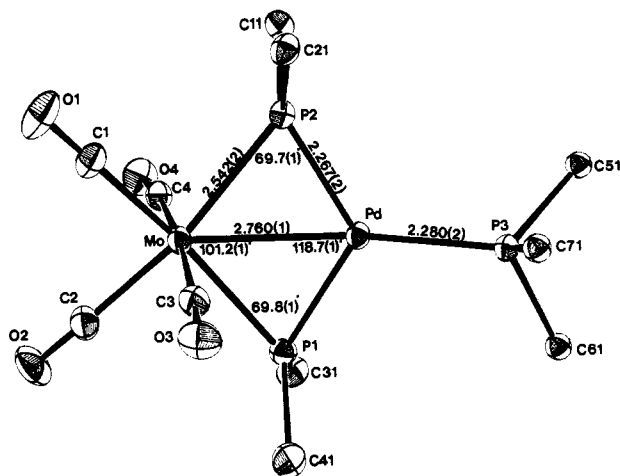
Figure 2. Perspective drawing of $(CO)_4Mo(\mu\text{-}PCy_2)_2Pd(PPh_3)$ (4) with only the non-hydrogen atoms and only the first carbon atom in each ring, showing some relevant bonding parameters.

The overall geometry of this dinuclear complex is a combination of the individual coordination geometries of the Mo and Pd atoms. The Pd atom is bonded to the three phosphorus atoms with an average Pd–P distance of 2.278 (8) Å. The largest deviation from the least-squares plane formed by the Pd and three P atoms is 0.0676 Å, and the P–Pd–P angles average 119.8 (1)°. This is consistent with a trigonal-planar geometry for Pd, if we neglect the Mo–Pd interaction. The Mo atom is bonded to the two bridging atoms (P1 and P2) and four carbonyl carbon atoms. The Mo–P distances are typical and average 2.536 (1) Å. The Mo–C distances average 2.03 (2) Å and also fall within the expected range. The C–Mo–C and P–Mo–C angles are consistent with a slightly distorted octahedral geometry about the Mo atom.

The $Mo(\mu\text{-}PCy_2)_2Pd$ core is not planar. The dihedral angle between the P1–Mo–P2 and P1–Pd–P2 planes is 15.4°, giving the molecule a very slight butterfly distortion. The Mo–Pd distance of 2.760 (1) Å is shorter than any yet determined:[17] $[\{PdNMe_2CH_2C_6H_4\}_2\{\mu\text{-}Mo(CO)_3(\eta\text{-}C_5H_5)\}\mu\text{-}Cl]$, 2.832 (1) and 2.788 (1) Å; $[Pd(8\text{-methylquinoline-}C,N)PPhMe_2Mo(CO)_3(\eta\text{-}C_5H_5)]$, 3.059 (1) Å; $[Pd_2Mo_2(\eta^5\text{-}C_5H_5)_2(\mu^2\text{-}CO)_2(PEt_3)_2]$, 2.827 (1) and 2.865 (1) Å. However, there are no comparable structures containing Mo and Pd and this distance is equal to the sum of the covalent radii.[18] As illustrated in Figure 2, other bond distances and angles in the $Mo(\mu\text{-}PCy_2)_2Pd$ core are consistent with a Mo–Pd bond. Also other workers have noted that, although the metal–metal interaction may be described as occurring through bridging phosphorus orbitals, a relatively short Mo–Pd distance of 2.760 (1) Å is not imposed by phosphido ligands.[19] The interaction is best described as a Mo(0) to Pd(II), polar, donor–acceptor bond:
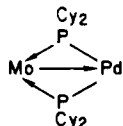
These formal oxidation-state assignments are consistent with spectroscopic and chemical observations and have been rationalized fully elsewhere for related phosphido-bridged complexes.[3]

The diphenylphosphido-bridged complex $(CO)_4W(\mu\text{-}PPh_2)_2Pt(PPh_3)$, recently characterized by an X-ray diffraction study,[3c] also contains a group 6 metal[20] and a group 10 metal

Chart I[a]
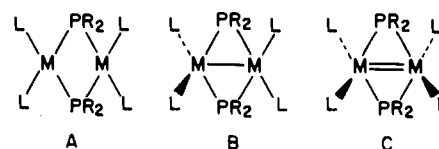
[a] L = CO, PR₃, etc.

bridged by phosphido ligands. A comparison with $(CO)_4Mo(\mu\text{-}PCy_2)_2Pd(PPh_3)$ illustrates the effect of replacing phenyl by bulky cyclohexyl groups as substituents on the bridging phosphorus atoms. The molecular structures of these two complexes are very similar, and the coordination geometries about the metal atoms are essentially identical. This is particularly true for the MM'-$(\mu\text{-}PR_2)_2$ cores, in which the bond lengths and angles show little difference; for example, the W–Pt bond distance[3c] is 2.764 (1) Å and the Mo–Pd bond distance is 2.760 (1) Å. The only major difference is the larger MM'$(\mu\text{-}PR_2)_2$ dihedral angle of 15.4° for 4 compared to 2.2° for $(CO)_4W(\mu\text{-}PPh_2)_2Pt(PPh_3)$.

Bulky substituents on the $M_2(\mu\text{-}PR_2)_2$ ring might be expected to produce a more planar structure since this would reduce steric interactions between adjacent R groups. Indeed, Jones has found that for the complexes $[Fe(\mu\text{-}t\text{-}Bu_2P)Cl(PMe_3)]_2$, $Co_2(\mu\text{-}t\text{-}Bu_2P)_2Cl(PMe_3)_2$, and $[Ni(\mu\text{-}t\text{-}Bu_2P)(PMe_3)]_2$, bridged by the bulky $t\text{-}Bu_2P$ ligand, the $M_2(\mu\text{-}PR_2)_2$ core is essentially planar.[6] However, 4 contains not only sterically demanding dicyclohexylphosphido-bridging ligands but also a relatively large ancillary triphenylphosphine ligand. The threefold symmetry of the PPh₃ group superimposed on the $Mo(\mu\text{-}PCy_2)_2Pd$ core results in steric interactions between phenyl and cyclohexyl groups. Ph6 is oriented between Cy3 and Cy4 (H32B–H62 = 2.532 Å; H42B–C61 = 2.967 Å), Ph5 is edge on to the face of Cy1 (H12B–H56 = 2.376 Å), and Ph7 is face to face with Cy2 (H26B–C76 = 3.035 Å). We presume therefore that the observed dihedral angle in the $Mo(\mu\text{-}PCy_2)_2Pd$ core occurs simply to minimize these group interactions. This does not occur for $(CO)_4W(\mu\text{-}PPh_2)_2Pt(PPh_3)$ since the PPh₂ ligands are less bulky and does not occur for the $t\text{-}Bu_2P$-bridged complexes mentioned, since the terminal ligands are relatively small. It should be noted, however, that this type of bridging–terminal ligand interaction can be very important. In the group 9 complexes $[M(\mu\text{-}PR_2)(L)_2]_2$ (M = Co, Rh, Ir), increasing the steric bulk of L increasingly favored C > B > A (Chart I).[7a]

Summary and Conclusions

The versatility of "bridge-assisted" synthesis for phosphido-bridged heterobimetallic complexes is demonstrated by its application to a series of dicyclohexylphosphido complexes that link Mo or W with Ni, Pd, and Pt. The substituion of cyclohexyl for phenyl groups adds stability as evidenced by the ease of preparation and characterization of the Ni complexes. This is probably due to a combination of increased basicity of the bridging P atoms and steric shielding by the cyclohexyl groups. It is hoped that the observed increase in steric interactions about the metal center might result in increased substitution rates and/or the generation of coordinative unsaturation. Also, it may be possible to obtain the specific activation of small molecules often observed for bulky trialkylphosphine complexes.[21] Studies on reactions of these types are under way and will be the topics of future publications.

(17) (a) Pfeffer, M.; Fischer, J.; Mitschler, A.; Richard, L. *J. Am. Chem. Soc.* **1980**, *102*, 6338. (b) Pfeffer, M.; Grandjean, D.; Le Borgne, G. *Inorg. Chem.* **1981**, *20*, 4226. (c) Bender, R.; Braunstein, P.; Dusausory, Y.; Protas, J. *Angew. Chem., Int. Ed. Engl.* **1978**, *17*, 596.
(18) Porterfield, W. W. *Inorganic Chemistry, A Unified Approach*; Addison Wesley: Don Mills, Ontario, Canada, 1983.
(19) See ref 3f and references therein.

(20) Periodic group notations are in accord with new IUPAC and ACS nomenclature.
(21) (a) Ibers, J. A. *Chem. Soc. Rev.* **1982**, *11*, 57. (b) Ritchey, J. M.; Moody, D. C.; Ryan, R. R. *Inorg. Chem.* **1982**, *22*, 2276. (c) Yoshida, T.; Thorn, D. L.; Okano, T.; Otsuka, S.; Ibers, J. A. *J. Am. Chem. Soc.* **1980**, *102*, 6451. (d) Kubas, G. J. *J. Chem. Soc., Chem. Commun.* **1980**, 61. (e) Kubas, G. J.; Ryan, R. R.; Swanson, B. I.; Vergamini, P. J.; Wasserman, H. J. *J. Am. Chem. Soc.* **1984**, *106*, 451.

is grateful for the award of an NSERC postgraduate scholarship.

Contribution from the Department of Chemistry,
York University, North York, Ontario M3J 1P3, Canada

Comparative Spectra and Kinetics of Ferrous Bis(dioxime) Complexes of π-Acid Ligands

Nafees Siddiqui and Dennis V. Stynes*

Syntheses, visible spectra, and kinetic data for axial ligand dissociation for low-spin *trans*-FeN₄XY complexes (N₄ = bis(benzoquinone dioxime) (BQDH), bis(naphthoquinone dioxime) (NPQH); X, Y = methylimidazole, tributylphosphine, tributyl phosphite, benzyl isocyanide, carbon monoxide) are reported and compared with corresponding dimethylglyoxime (DMGH) analogues. MLCT bands in both NPQH and BQDH derivatives are red-shifted up to 200 nm from those in corresponding DMGH complexes, and all show shifts as a function of axial ligands that correlate with π-acceptor character. Infrared data and CO dissociation rates indicate an axial π-back-bonding order DMGH > NPQH > BQDH. The NPQH complexes have labilities comparable to those of DMGH analogues but several orders of magnitude slower than those of BQDH complexes. All three systems give the trans-effect series MeIm > PBu₃ > P(OBu)₃ > BzNC > CO (except PBu₃ > MeIm for BQDH complexes). The three systems provide a set of over 50 different complexes whose dissociative thermal substitution reactions are fully characterized and that display photochromism based on photochemical substitution in solution covering the entire visible region of the spectrum.

Introduction

Kinetic investigations of axial ligand substitution in a variety of low-spin iron(II) complexes of the general form *trans*-FeN₄LT, where N₄ is a planar tetradentate ligand and L and T are monodentate ligands, have established a dissociative mechanism. The system N₄ = bis(dimethylglyoxime) has been the most extensively studied, and correlations in reactivity with the MLCT band have been observed.[2,3] An analogous benzoquinone dioxime system[4] displays a 200-nm shift of the MLCT band and exhibits kinetic and spectroscopic properties for carbonyl and isocyanide complexes that are substantially different from those of the DMGH analogues. Previous studies of naphthoquinone dioxime complexes of iron without consideration of the axial ligands present have been reported.[5-7]

Herein we present a comparison of the spectroscopic and kinetic parameters for benzoquinone dioxime, naphthoquinone and dimethylglyoxime complexes containing methylimidazole, pyridine, tributylphosphine, tributyl phosphite, benzyl isocyanide, and carbon monoxide as axial ligands. A systematic analysis of the labilization effects in these three systems provides a basis for understanding the reactivity of low-spin d⁶ complexes and insight into the even greater lability of hemes.

BQDH   NPQH
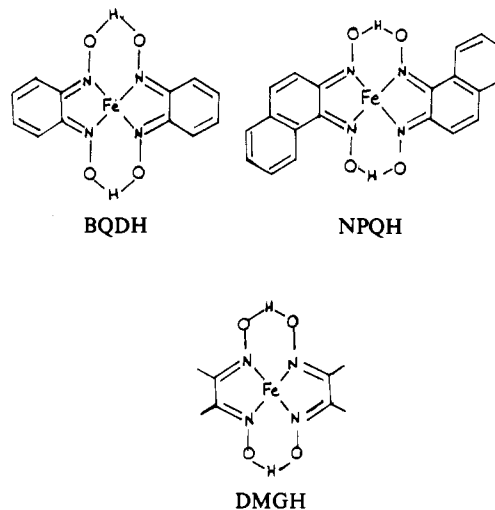
DMGH

Results and Discussion

Data for the BQDH and NPQH complexes generally follow trends similar to those for the DMGH system described in detail previously.[2] Species show characteristic MLCT spectra, and axial ligand substitution reactions are readily followed by visible spectroscopy, providing overwhelming evidence for a classic dissociative mechanism. The rate constants, all obtained in toluene solution, provide fundamental information about the metal–axial ligand bonding and its dependence on the *cis*-N₄ ligand and trans ligand. Activation parameters show these effects to be largely enthalpic and not very sensitive to solvation effects.

Visible Spectra. The visible spectra of iron bis(dioxime) derivatives are dominated by an intense MLCT band assigned to metal d(*xz*,*yz*) to oxime charge transfer.[8] Substantial shifts in this band are observed as extended conjugation in the oxime ligand

(1) Abbreviations: DMGH, dimethylglyoximate; BQDH, benzoquinone dioximate; NPQH, naphthoquinone dioximate; MeIm, 1-methylimidazole; Im, imidazole; BzNC, benzyl isocyanide; TMIC, (*p*-tolylsulfonyl)methyl isocyanide; py, pyridine; 4-CN-py, 4-cyanopyridine; 3,4-Me₂-py, 3,4-dimethylpyridine; 4-Me₂N-py, 4-(dimethylamino)-pyridine; MLCT, metal to ligand charge transfer. Rate constants are designated by k^T_{-L} for dissociation of the ligand L trans to T. The shortened forms N (MeIm), P (PBu₃), and PO (P(OBu)₃) are used as subscripts and superscripts.
(2) (a) Pang, I. W.; Stynes, D. V. *Inorg. Chem.* **1977,** *16,* 59. (b) Chen, X.; Stynes, D. V. *Inorg. Chem.,* in press.
(3) Vaska, L.; Yamaji, T. *J. Am. Chem. Soc.* **1971,** *93,* 6673.
(4) Pomposo, F.; Stynes, D. V. *Inorg. Chem.* **1983,** *22,* 569.
(5) Toel, K.; Motomizu, S.; Kuse, S. *Anal. Chim. Acta* **1975,** *75,* 323.
(6) Marvel, G. S.; Porter, P. K. *Organic Syntheses;* Wiley: New York, 1950; Collect Vol. II, p 411.
(7) Nasakkala, M.; Saarinen, H.; Korvenranti, J.; Nasakkala, E. *Acta Chem. Scand., Ser. A* **1977,** *A31,* 469.
(8) Yamano, Y.; Masuda, I.; Shinra, K. *Bull. Chem. Soc. Jpn* **1971,** *44,* 1581.